Advancement in experimental methodologies to produce phase equilibria and thermodynamic data in multicomponent systems

M. Shevchenko [1], Denis Shishin [2], and E. Jak [3]

1. Research Fellow, PYROSEARCH, University of Queensland, Brisbane, QLD, 4072. Email: m.shevchenko@uq.edu.au
2. Research Fellow, PYROSEARCH, University of Queensland, Brisbane, QLD, 4072. Email: d.shishin@uq.edu.au
3. Professor, Centre Director, PYROSEARCH, University of Queensland, Brisbane, QLD, 4072. Email: e.jak@uq.edu.au

ABSTRACT

One of the key aspects to develop sustainable metallurgical production is to ensure that the predictive power of thermodynamic tools is brought up to a new level of accuracy and reliability. Exploring new polymetallic processes, integrating primary and recycled materials, means utilizing the uncharted areas within the Cu-Pb-Zn-Fe-Ca-Al-Mg-Si-O (major) – Cr-Na (slagging) – As-Sn-Sb-Bi-Ag-Au-Ni-Co (minor) slag-solids-metal-matte-speiss-sulphate system. This requires extensive integrated experimental and thermodynamic modelling study, which is underway at PYROSEARCH (UQ).

Recent improvements in experimental methodology allowed: a) generating over a thousand equilibrium data points per year by high-temperature (400-1750°C) equilibration, quenching, Electron Probe X-ray Microanalysis (EPMA) technique at laboratory-controlled oxidation/reduction conditions; b) studying previously impossible systems by smart choice of substrates corresponding to system conditions, one example being rhenium foil for Sn- and Sb-rich slags, c) systematic updates in the properties of pure components/endmembers to provide self-consistent heat capacities from -273 to >3000°C in all phases, enthalpies of phase transition and melting points.

The accuracy of measurements also increased. For instance, selected compounds with well-known stoichiometry were systematically used as a set of secondary standards. Also, effects of secondary X-ray fluorescence were addressed. As the experimental techniques improve, new areas of compositions are revealed, which are not necessarily easy to describe using the existing thermodynamic model frameworks. Examples of these areas are: miscibility gaps in silicate systems, many of which never accurately measured before; multicomponent 4-phase liquid equilibria slag-matte-metal-speiss; liquidus temperatures for extremely high melting oxides CaO, MgO, NiO and SnO_2.

INTRODUCTION

Pyrometallurgy is an important sector of modern industrial society actively participating in solving current environmental, economic, materials scarcity and other challenges (Jak 2018). Fundamental theoretical models can now be used to make a significant next step towards the development and implementation of computerised models describing real industrial processes. Recent trends determine the new challenges for the scientists including a) stricter demand for the accuracy of the data, and b) more difficult systems for research and c) more components of chemical systems (Jak 2012). The ultimate target is development of "Pyro-GPS" multicomponent, multi-phase, wide range of conditions thermodynamic model (Jak et al. 2024).

An outline of the fundamental and applied research, through the expert analysis of processes of the industrial processes, to the implementation of the results of the research outcomes into industrial operations, was provided by (Jak 2012). The present paper attempts to present the developments of this approach that happened during the last 12 years. The integrated experimental/thermodynamic modelling approach developed in previous studies by the co-authors (Jak, Hayes, and Lee 1995; Jak 2012; Jak et al. 2016), based on microanalysis of equilibrium phase compositions, represents a breakthrough in the accuracy, productivity and range of conditions to be studied (Jak et al. 2024).

New experiments are essential for development of the new model. Literature lacks both cover of systems/conditions and often accuracy. Experiments need to be planned to ensure sufficient (1) quantity and coverage of systems and conditions; (2) accuracy and reliability.

(1) Which systems to investigate and how densely?

The range of characterised systems keeps extending each year. Due to large scope of possible studies (thousands of binary, ternary and quaternary systems, with 10-200 experiments potentially needed in each), it is essential to identify priorities and conduct minimum sufficient number of them in the most important systems first (Jak et al. 2024). This planning is driven by the model requirements – experiments location and quantity should adapt to the model needs.

Since most models in the currently available thermodynamic software packages have only binary and ternary parameters, it is essential to study all corresponding binary and ternary systems ("no experiments – no parameters" approach). Importantly,

- Thermodynamic data for pure components – H, G, S, Cp(T) for all stable and metastable phases (e.g. supercooled liquids as endmembers for slag) – are often not reliable due to high melting points (>2000°C: CaO, MgO, Al_2O_3, Cr_2O_3, SnO_2), instability (Ag_2O, Au_2O), volatility (As_2O_3, Sb_2O_3, SnO, ZnO), extreme reactivity (Na_2O), etc. Therefore, binary and often ternary or even quaternary data are needed just to understand the behaviour of pure components properly.

- Similarly, some areas of binary systems are not known directly. But they are required for description of ternary and higher-order systems – that is how the models work. Although ideally it would be desirable to have 20-30 reliable points in each binary system (at least one point per each 5 mol.%), this can rarely be achieved in practice due to a) high liquidus temperature of many areas, particularly close to pure components, that exceeds the current technique limits (1750 °C); b) instability, volatility and reactivity of pure components as listed above; c) inability to quench liquids with compositions rich in some of the components that are poor glass-formers – particularly metals.

E.g. FIG 1 for $CaO-NiO-SiO_2$:

SiO$_2$

large uncertainty
(miscibility gap,
T>1750°C)

unknown
(miscibility gap,
T>1750°C)

well known

known

large uncertainty
(1750-2100°C)

unknown
(T>1750°C)

unknown
(T>2100°C)

CaO
T$_{melt}$=2900?

unknown
(T>1750°C)

known

NiO
T$_{melt}$=1990?
Or decomposition to Ni+O$_2$?

FIG 1 – Example of limited binary thermodynamic data for the CaO-NiO-SiO$_2$ system.

A random composition inside the area of realistic liquid slag, is shown using the blue dot in FIG 1. For this composition, thermodynamic properties are calculated by combining properties from three binaries as shown by the blue arrows, with further addition of ternary parameters. It is very likely, interpolation into ternary system is done from the unknown part of a binary sub-system. That is why ternary data may and should be used to double-check and evaluate the properties of binaries in the areas that cannot be studied directly.

Similarly, not all areas of each ternary system can be directly studied, but they may be revealed by experiments in the certain quaternary systems. Thus, quaternary systems must be studied and used to test the values of binary and ternary parameters.

Furthermore, a third or fourth component can sometimes be used as a flux added to the binary (or ternary) eutectic, to study the subsolidus behaviour in a more productive way. For instance, kinetically-limited solid-state experiments within the MgO-AlO$_{1.5}$-SiO$_2$ system would likely result in a sample, which is porous, contains compositional gradients, and very hard to polish into smooth surface. For this system, the phases are also indistinguishable due to similar brightness in back-scattered electron image, which relies on the difference in average atomic numbers of phases. Alternative approach involves the addition of PbO flux, as shown in FIG 2. PbO does not form any solid solutions with MgO-AlO$_{1.5}$-SiO$_2$ phases, neither it forms new stable solid phases. The addition of even small concentration of PbO to the liquid slag immediately makes it much brighter than all solids, giving the necessary contrast for effective sample much analysis. Some ternary invariant points involving slag have too high temperature to be studied directly. For instance liquid slag-lime-periclase-C$_3$S equilibrium within the CaO-MgO-SiO$_2$ system has the temperature of >1800°C. An addition of a fourth component, such as AlO$_{1.5}$, extends this invariant point as a lower temperature univariant line, allows measuring phase compositions accurately, and then extrapolate the quaternary results to obtain the compositions of all liquid and solid solutions in that point for the AlO$_{1.5}$-free ternary system.

FIG 2 – Example microstructure of approaching the MgO-AlO$_{1.5}$-SiO$_2$ system (tridymite-pyroxene-cordierite solids) by addition PbO-rich flux (slag), and CaO-MgO-SiO$_2$ (lime-periclase-C$_3$S solids) with AlO$_{1.5}$ liquid slag.

High-order systems (4-, 5-, 6-component, etc.) are the ultimate target for thermodynamic predictions, relevant to the industrial purposes. The predictions must be confirmed by a certain number of experiments, preferably covering a large volume of the multidimensional compositional space. Traditional binary and ternary diagrams cannot represent the results of calculations and experiments in such systems. Several options exist to represent and analyse phase equilibria in these cases:

- Pseudoternary sections, where the concentrations or ratios of all components except three are fixed. Example: for the 6-component (PbO+CaO+SiO$_2$)-FeO-Fe$_2$O$_3$-ZnO systems, the ratio PbO/SiO$_2$ and CaO/SiO$_2$ can be fixed, furthermore the p(O$_2$) is fixed at 0.21 atm to define the FeO/Fe$_2$O$_3$ ratio, allowing the (PbO-CaO+SiO$_2$)-(FeO+Fe$_2$O$_3$)-ZnO pseudo-ternary diagram (Jak and Hayes 2002b, 2002a).

- Projections from the selected apex(es) of the multidimensional space. In the FactSage calculation, this can be achieved by fixing the activity of the corresponding primary solid phase to 1, and analysing the secondary phase fields (Shevchenko and Jak 2020b; Wen et al. 2023).

- Plotting the phase diagram based on three major components and analysing the behaviour (solubility, activity coefficients) of other minor components (Shevchenko, Chen, and Jak 2021).

Types of thermodynamic data

For each system, multiple types of thermodynamic data exist:

- Properties (H, G, S, Cp, vapour pressures, etc.) of pure components, compounds and solutions as functions of temperature, most importantly $\Delta_f H°_{298}$, $S°_{298}$.

- Properties of compounds and solutions (liquid, solid) as functions of temperature: integral and partial H, G, S, activities of components, vapour pressures.

- Phase equilibria: liquidus of each phase; extents of solutions; special points / lines of phase diagrams (phase transitions, eutectics, univariants, etc.); distributions of elements between phases.

Only rarely, all these types of data are available and even possible to measured directly. Lack of some types of data can be partially compensated by improved reliability and range of other types.

Current scope of study by PyroSearch team

Wide range of objects is studied simultaneously by the PyroSearch team: slag (including silica-free and other "exotic" systems), matte, metal, speiss, liquid sulphates, solid solutions (FIG 3). Attempts are taken to develop other techniques: DTA/DSC, viscosity, electrical conductivity, aqueous leaching.

4
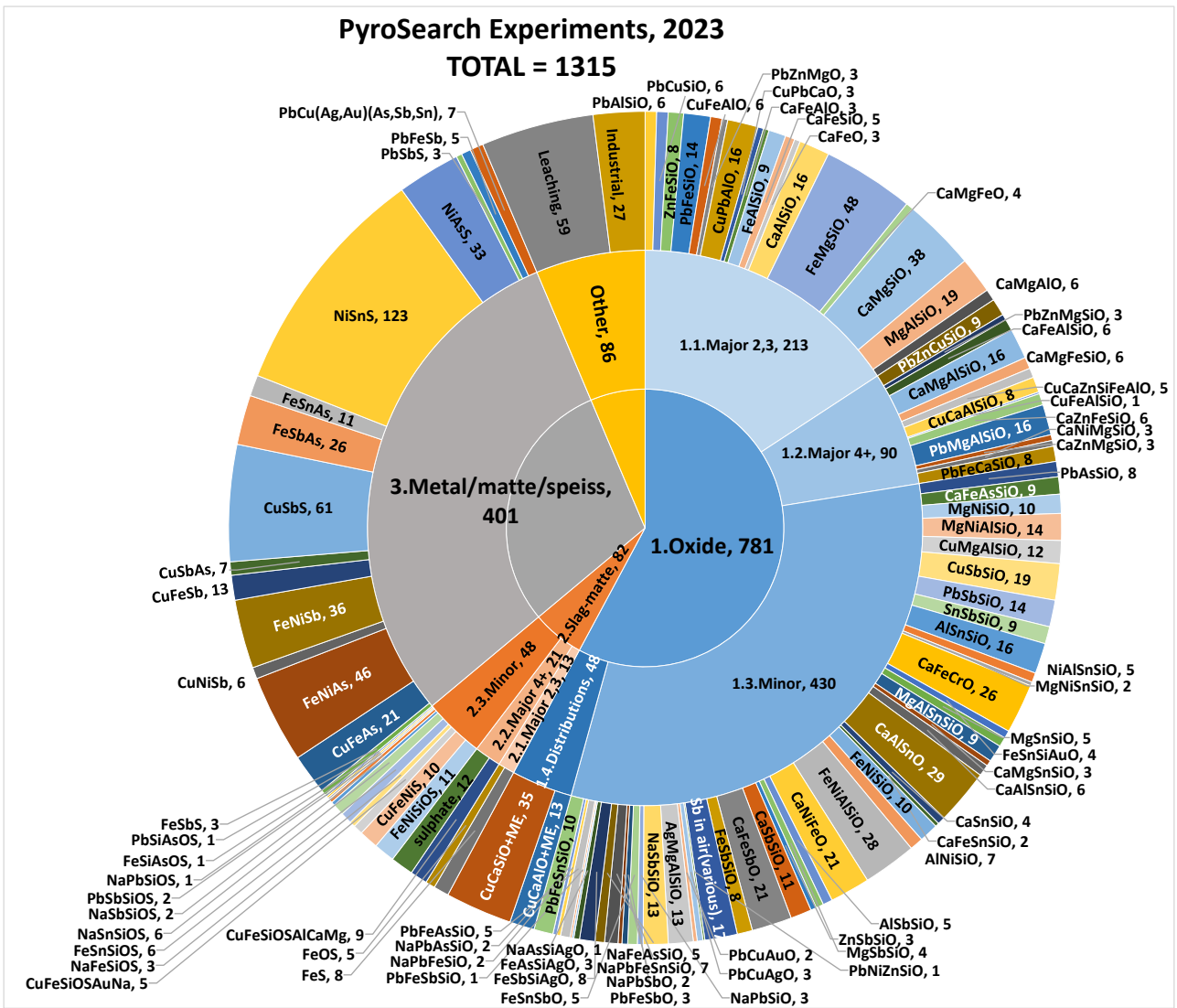
FIG 3 – Summary of all successful experiments done at PYROSEARCH in a typical year (2023).

Examples of microstructures of quenched high-temperature samples obtained in recent years are shown in FIG 4.

FSSCA3-1300: slag (Ca-Al-Si-O), matte (Fe-S), Fe, tridymite

PCSbAu4-510 / matte, copper, tridymite crystals, willemite, slag

PbFeSb1-1010: Pb-Sb metal, Fe-Sb speiss, Fe(bcc), liquid Pb, (Cu,Au)₃Sb, liq-speiss, fcc

PCAsAg5-600: liquid metal, liquid speiss, Cu-Ag(fcc)

PCAsAu3-745: liquid metal, speiss, Cu₃As, slag, quartz

6
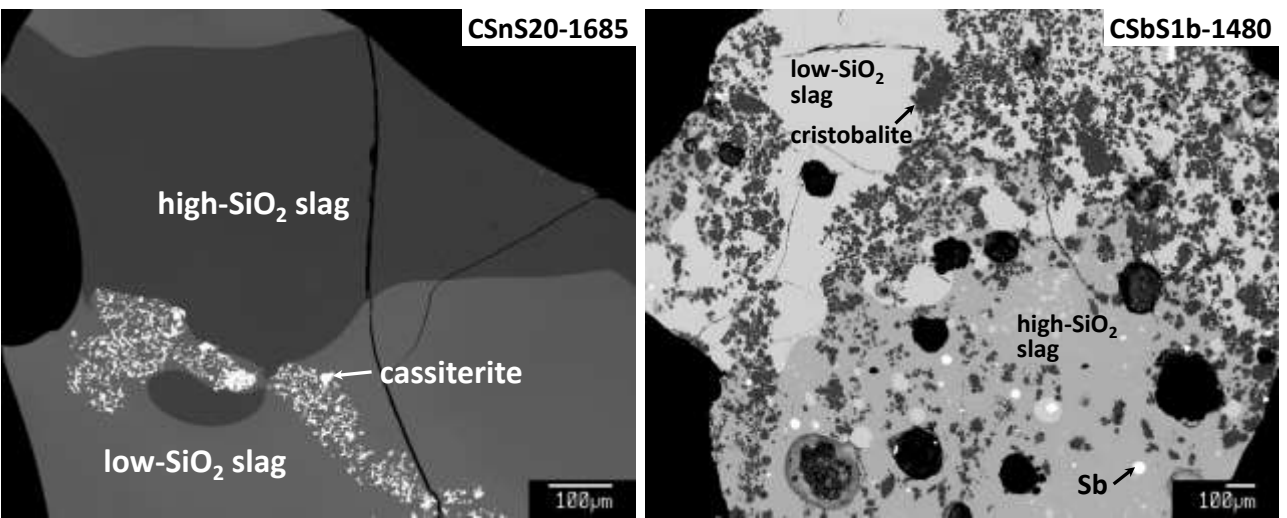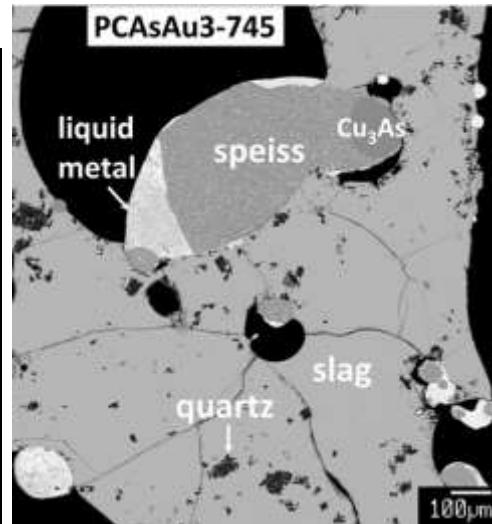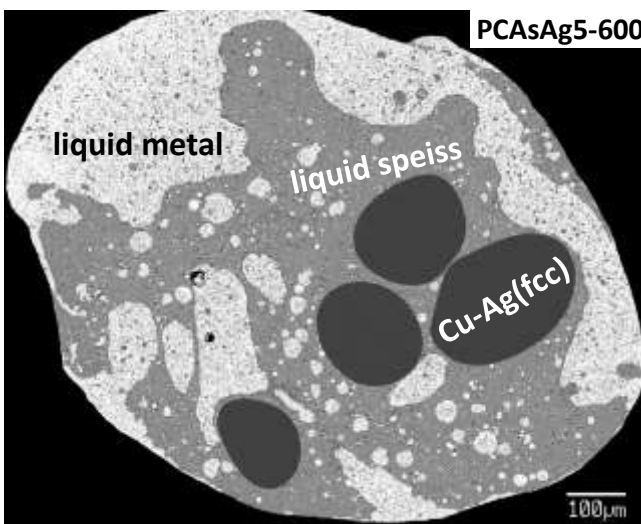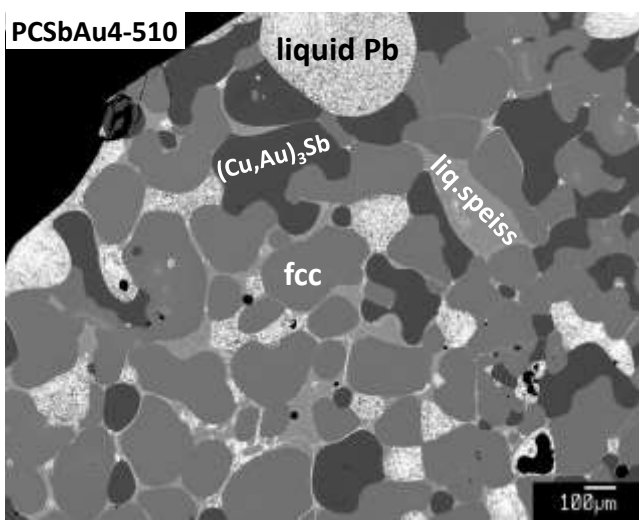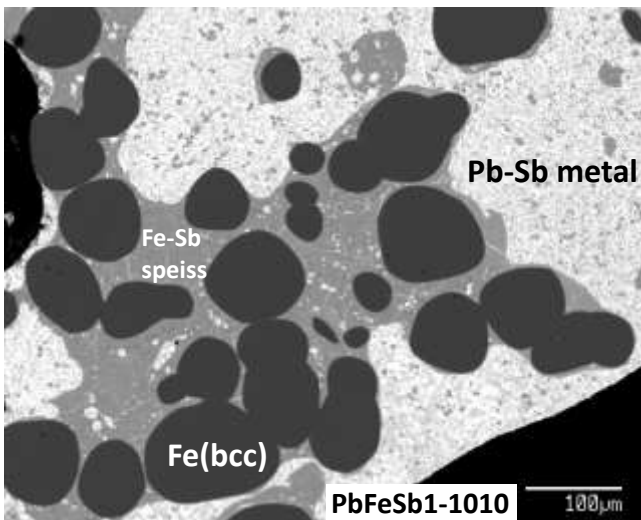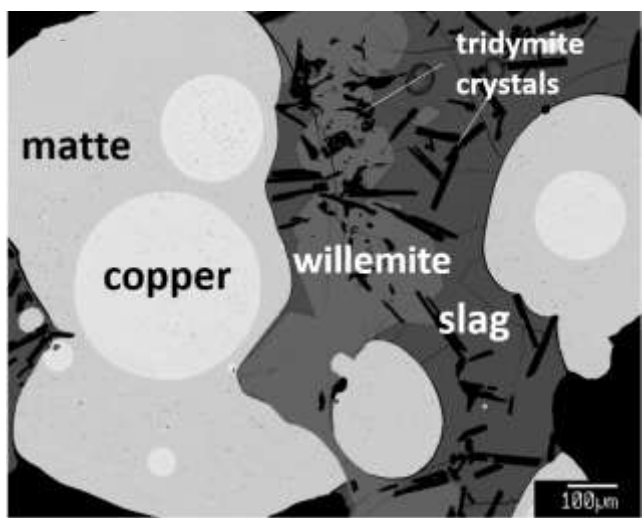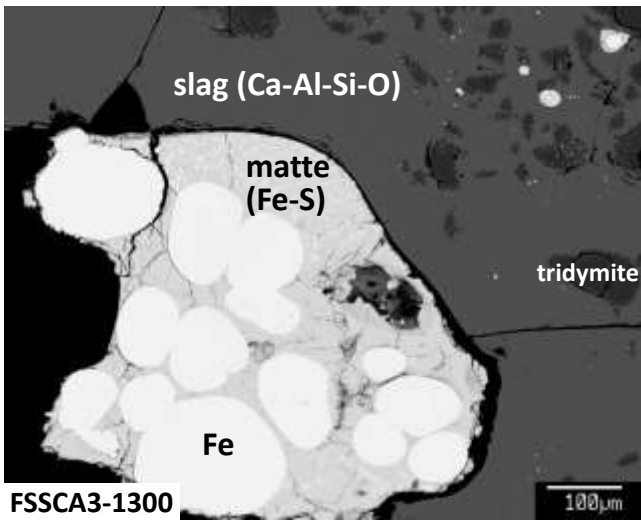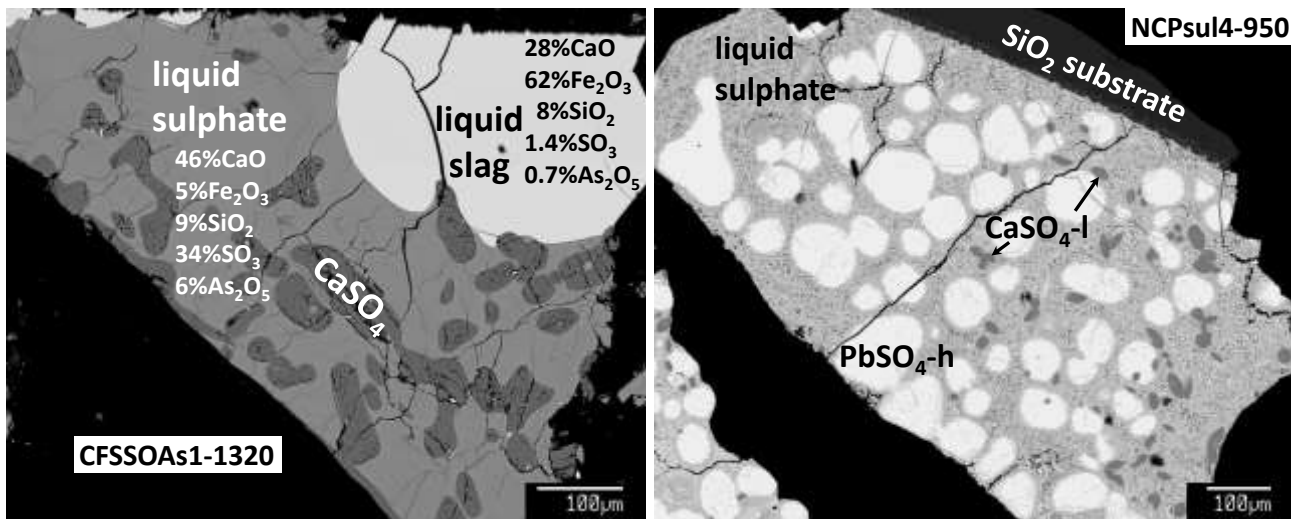
FIG 4 – Examples of microstructures in various types of systems studied at PYROSEARCH: immiscible liquid slags; liquid slag-matte-metal; metal-matte-speiss; metal-speiss-solids-slag; liquid sulphate-slag-solids.

(2) Accuracy and reliability of experiments.

Although the equilibration, quenching, electron probe X-ray microanalysis proved to be powerful, and seem easy to implement, there is a long list of possible issues that can lead to experiment failure or unreliable results. Each time a new type of object is studied, it is essential to prove that sample has reached equilibrium and that its quenched state properly represents that high-temperature equilibrium. Multiple stages of each experiment need a careful approach to avoid uncertainties, including:

- Experimental: impurities, achievement of equilibrium, temperature and gas composition uncertainties, quenching quality.

- Analytical: selection of area for analysis, effect of probe diameter, standards, characteristic line selection and interference, ZAF-correction, beam-sensitive elements, secondary fluorescence.

2.1. Conditions: accuracy of temperature, $p(O_2/SO_2/etc.)$, stability of substrates, absence of impurities. The impurities can be introduced from original materials, during the sample preparation, during the equilibration in impure atmosphere / dust, due to reaction with substrate, and at post-quenching treatment due to hydration, oxidation.

A large variety of the starting materials is used:

- Pure powders, e.g. Fe, FeO_{1+x}, Fe_3O_4, Fe_2O_3, FeS, Cu, Cu_2O, CuO, Cu_2S, $CaCO_3$, CaO selected by optimising the purity, mixing efficiency, availability, price-to-value ratio.

These can be affected and controlled by:

- Reactions during heating / melting. For instance, CuO can de-compose upon heating, iron and lead oxides will react according to $Fe + PbO = FeO + Pb$,

- A thermal arrest at lower than target temperature, e.g. to melt a mixture of $PbO + SiO_2$, or Cu + As.

Master slags / matte / speiss are often prepared in advance. The PbO-SiO_2 master slag is necessary to minimise vaporisation of PbO in initial stages of experiment. The CaO-SiO_2, $Ca_2Fe_2O_5$ need to be prepared to avoid residues of volatiles, $CaCO_3$ and $Ca(OH)_2$. Without complete removal of volatiles, sealed ampoule experiment can fail due to expansion. The synthesis of compounds like Cu_3As, FeAs, SnS, Sb_2S_3 may help avoiding the conditions where combined pressure of arsenic-sulphur containing gaseous species exceeds 1 atm and results in explosion.

The selection of a holding material for the sample equilibration is not straight forwards. Over the years, many combinations substrates and samples has been developed at PyroSearch, which are summarized in TABLE 1 and FIG 5. Substrates made of "inert" precious metals requires careful

analysis of experimental conditions. Factors, such as temperature, $p(O_2)$, and possible reactions with corrosive metals, such as Cu, Pb, Sn, Sb, etc., their oxides and mattes, often make them impractical to use. Both the melting points and the affinity for oxygen of most commonly used precious metals increase in the order Au < Pt < Ir < Re (Jak et al. 2022).

TABLE 1 – List of substrates applied at PYROSEARCH for high-temperature phase equilibria studies.

Material	Advantages	Disadvantages	Systems studied, examples
SiO$_2$ ampoule	Allows full protection from interaction with gas and evaporation of volatile materials. Used for quartz, tridymite, cristobalite liquidus, or others if second substrate enclosed inside:	Sometimes infiltrated by slag (e.g. FeO-rich). Can expand and block the furnace at high T if any gas is released from sample.	Preferred for all oxide systems (high-SiO$_2$ ranges) where contact with gas is not needed. Also – slag-matte-metal, matte-metal-speiss...
SiO$_2$ ampoule with a hole	Allows the escape of released gas (CO$_2$, O$_2$, SO$_2$) and exposure to outside gas, which is not too far from composition inside.	The equilibration with gas is not fast enough in some cases.	Pb slag-matte-metal at high pSO$_2$ – limits evaporation of Pb. Fe-Sn-Si-O at high pO$_2$.
SiO$_2$ open crucible	Allows faster equilibration with gas (e.g. CO-CO$_2$)	Exposes a sample to dust contamination from above.	Large range of slag-metal, slag-metal-matte at fixed pO$_2$.
Al$_2$O$_3$ crucible	Strong, not expensive, available in multiple sizes. Can be enclosed in SiO$_2$ ampoule (up to 1590°C) for volatile systems.	Relatively thick, may prevent fast quenching. May be infiltrated by slag.	Cu-Ca-Al-O
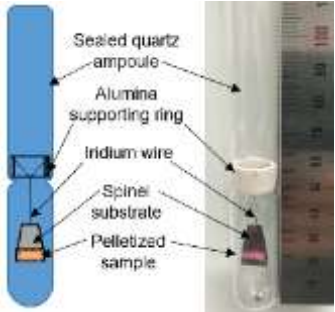
MgO crucible 	Low solubility in most silicate, Cu- and Pb-slags. May be covered by protective layer of olivine. Can be enclosed in SiO_2 ampoule (up to 1540°C) for volatile systems.	Thick, may prevent fast quenching. May be infiltrated by slag. Contains ~3% Y_2O_3 impurity. Relatively brittle and expensive.	Cu-Mg-Si-O, Pb-Mg-Si-O
Au foil 	Very stable to oxidation to slag, does not form any oxide compounds. Reusable.	Low T_{melt} = 1064°C, even lower in presence of Pb, Sn, Sb, ...	PbO-rich slags at low T
Pt foil/wire/ crucible 	Easy to manufacture, thin – promotes fast quenching. Does not oxidise in air in contact with most slags.	Can form liquid or solid alloy in presence of Pb, Sn, Sb, Ni, Fe... at high T and reducing conditions. Can oxidise to slag (up to 0.3 wt.%) or compounds (Pb-Pt-O, Ca-Fe-Pt-O) at low T and high $P(O_2)$. Expensive, not reusable.	Ca-Fe-Si-O, Pb-Fe-Si-O, etc.
Pt-25%Ir foil 	Stronger than Pt, and less brittle than Ir, therefore reusable. High T_{melt} than Pt.	Intermediate resistance to alloy formation (reducing) and oxidation to slag/compounds between Pt and Ir.	Preferred for most oxide systems in air or mildly reducing / inert atmosphere.
Ir wire/plates 	Stable to corrosion by Cu, Pb, Sn metals.	Can oxidise to compounds (Pb-Ir-O, Ca-Ir-O, spinel...) at low T and oxidising conditions Relatively brittle. Expensive, not reusable. Plates are particularly expensive but reusable.	Cu, Pb, Sn systems. The only substrate to work in air above 1750°C, and in reducing atmosphere + corrosive metals.
Re foil/wire 	Stable to corrosion by liquid Cu, Pb, Sn, Sb, Bi, Ag, Au metals. Not brittle, reusable.	Can oxidise to slag, oxide compounds, and gas (e.g. in air it just gradually burns out).	SnO- and Sb_2O_3-rich systems in equilibrium with metal

Ag wire	Easy to manufacture.	Low T_{melt} = 962°C. Easily oxidises to slag.	Pb-Ag-Si-O
Pd wire	Similar to Pt, may be less prone to formation of certain oxide compounds, e.g. calcium ferrites.	Lower T_{melt} than Pt and higher solubility in most slags.	Ca-Fe-O
Mo, W wire	Very high T_{melt}, strong, not expensive.	Easy to oxidise and contaminate slag, form many stable solid compounds. Also form volatile MoO_3, WO_3 which cause persistent furnace contamination. Only for very reducing conditions.	Fe-Mg-Si-O
Cu foil/wire	Cheap, easy to manufacture.	T_{melt} = 1085°C, further reduced by impurities.	Cu-Pb-Si-O
Ni foil/wire	Cheap, easy to manufacture.	T_{melt} = 1455°C, further reduced by impurities.	Ca-Ni-Al-O
Co foil/wire	Cheap, easy to manufacture.	T_{melt} = 1495°C, further reduced by impurities. Requires careful protection from oxidation.	Co-Si-O
Fe foil/wire	Cheap, easy to manufacture	Requires careful protection from oxidation. Wetted by slag and liquid metals that creep into thin layer. Usually has some Mn contamination (~0.1%) that preferably goes to slag.	Ca-Fe-Si-O, Pb-Fe-Si-O (reducing – equilibrium with Fe)
FeO, Fe_3O_4 prepared from Fe foil/wire	Can be reliably manufactured. Good choice for corrosive slag-metal combinations.	Brittle, very porous. Slag can be fully lost into pores. Not as good when slag has spinel-forming components (Al, Mg, Zn, Ni) – unclear if slag-spinel equilibrium distribution is reached.	Cu-Ca-Fe-O, Cu-Fe-Si-O, Pb-Fe-Si-O spinel and wustite liquidus

Other sintered oxides (CaSiO₃, ...)	Can be used in primary phase fields of respective compounds, when all other substrates are too reactive.	Brittle, very porous. Slag can be fully lost into pores. Complicated preparation with low success rate. Still requires other intermediate substrates (metal wires) for handing.	Cu-Ca-Si-O
Future plans – Cr₂O₃	Very low solubility in most silicate slags, high T_{melt}.	Technique requires development.	Cr systems, multicomponent Pb slags
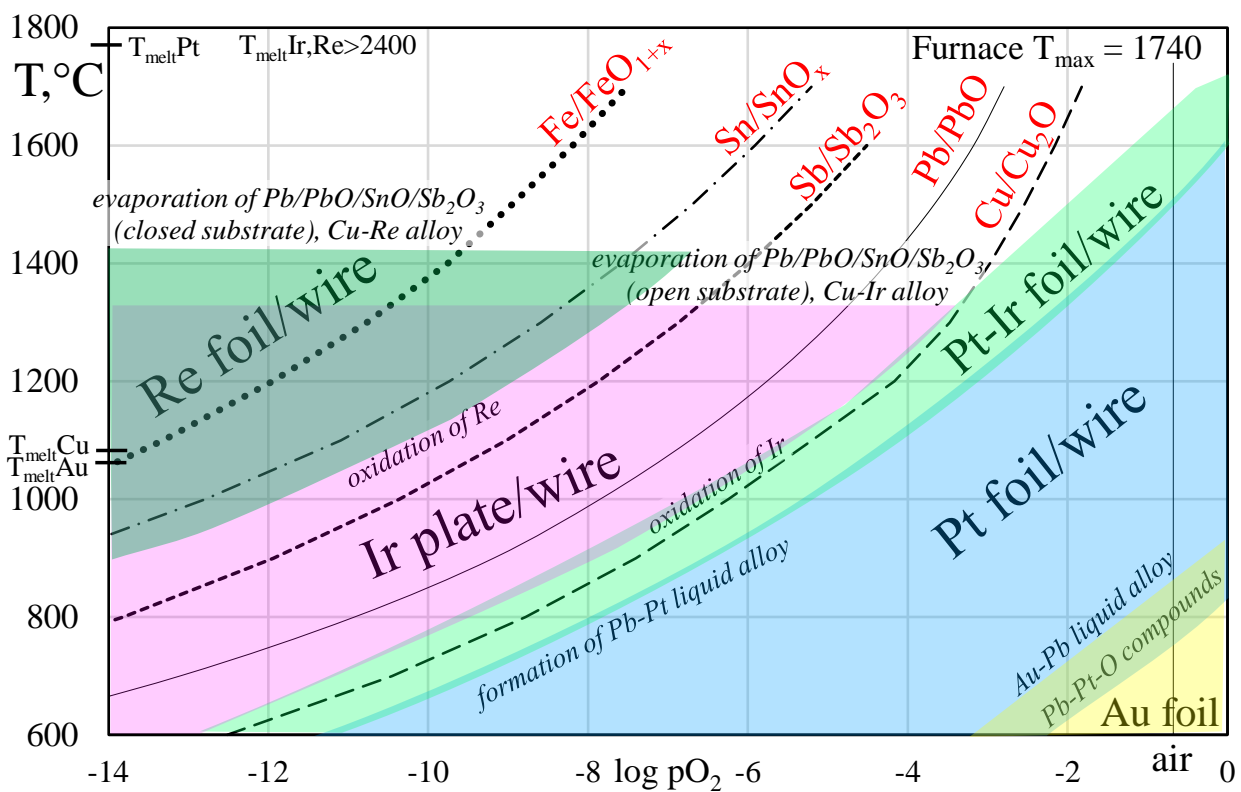
FIG 5 – Typical substrate preferences depending on pO_2 and T (Jak et al. 2022).

2.2. Achievement of equilibrium: completion of reactions. General principles: macro- and micro-inhomogeneities, fast (liquid/solid) vs slow (gas/liquid, solid/solid) reactions.

Confirmation of achievement of equilibrium can be complicated, formulated as a "4-point test" (Jak 2012; Shevchenko et al. 2016) including: (1) variation of equilibration time; (2) assessment of the compositional homogeneity of the phases by EPMA; (3) approaching the final equilibrium point from

different starting conditions; and, importantly, (4) consideration of reactions specific to this system that may affect the achievement of equilibrium or reduce the accuracy.

- Direction of reactions towards equilibrium – should be investigated in preliminary experiments to avoid blocking mass transfer during equilibration (Hidayat et al. 2023).

- Distance to equilibrium point:
  - in initial experiments can be larger to ensure approach to equilibrium from different directions;
  - final experiments – better to be in the "believed to be true".

Planning may be assisted with FactSage with adjustment for "believed to be true", but also can be done with a separate "mass balance" model.

Preliminary short experiments (1-5 minutes) are recommended at the initial stage of study of each system, to identify most important reactions on melting. Final equilibration time can vary from 10-15 minutes (very high temperature ~1700-1750°C, fluid low-SiO_2 liquids, presence of volatile components such as ZnO, SnO_2) to 2-24 h (typical) and even several weeks (low temperature ~500-700°C, viscous liquids rich in SiO_2, PbO, Sb_2O_3, expected slow-forming compounds such as $PbSiO_3$).

2.3. Quenching.

Selection of quenching medium. The best is not "as cold as possible" but "as far from boiling point as possible, in terms of enthalpy". E.g. liquid N_2 is very cold but close to the boiling point, and thus a very bad quenching medium. Sometimes, is referred to as Leidenfrost effect. Water at room temperature is not as good as water at 0°C. Even better is the salt brine at -20°C. It is not just the low temperature, but also the prevention of continuous vapour cushion blanket due to the change in regime of boiling (Pizetta Zordão et al. 2019; Luty 1992). Other possible, but less used quenching media is fluororganic liquid NOVEC1230, $C_6F_{12}O$, also known as "dry water", which is applicable samples that are water-sensitive, such as high-Na_2O slags and molten salts. Oils are not used for quenching due to fire hazard and because the oil contamination is very bad for the electron microscopes.

Depending on the properties of phases and their combinations, the main uncertainty is either the achievement of equilibrium or preservation of equilibrium during the quenching (FIG 6). The former is limiting for highly viscous liquids or slow solid-state reactions, while the latter is a problem for very fluid liquids, or reactions happening fast at temperature drops.

| | Hardest to quench/ Easiest to reach equilibrium | | | | | Easiest to quench/ Hardest to reach equilibrium | |
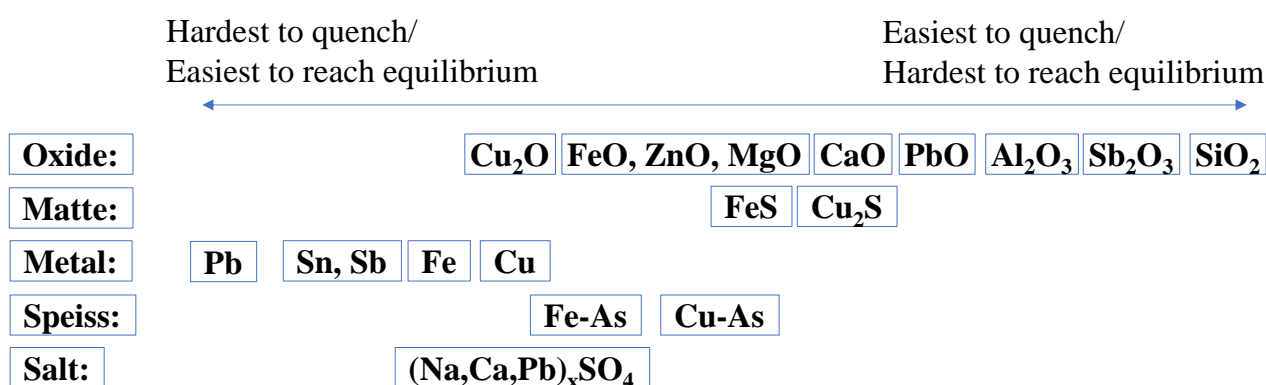
FIG 6 – Approximate rating of liquids by behaviour on quenching.

- Fluid liquid – expected problems with quenching and no issues with equilibration – % solids should be minimum with maximum liquid exposed first to the quenching media and later found in the mounted sample, equilibration time can be shorter (unless gas is involved)

- Viscous liquid – expected problems with equilibration and no issues with quenching - % solids should be higher, but not blocking mass transfer access to other phases (e.g. gas, matte, slag)

2.4. Analysis of phase compositions. EPMA is the main technique – allows high accuracy after taking all necessary precautions:

Selection of area for analysis. It is recommended to avoid immediate proximity to solids, dendrites and micro-inhomogeneities. Areas closer to surface provide better quenching (FIG 7). Good areas must have all needed phases to be present within the diffusion path. When some expected phases are lacking in the area, it is sometimes referred to as macro-inhomogeneities. A number of separate areas in sample should be investigated. Within each area, at least 5 points should be measured for well-quenched samples and 15-20 for poorly quenched. Also, for poorly quenched samples, a non-zero probe diameter is selected, within the 20-100 micron. This helps to average minor local micro-inhomogeneities formed during the quenching.

The volume fraction of solids is targeted to be below 50%, and preferably about 10%, to achieve rapid equilibration and satisfactory quenching of the liquid phase into an amorphous material. The solid phases act as heterogeneous nucleation centres, and a minimum distance of 10-20 μm between solid grains is necessary to ensure that an amorphous slag of uniform composition exist between the grains. In this case, it is unaffected by dendritic crystal growth during quenching. The correlation between the volume fraction of the solid phases and the volume fraction of the liquid slag phase affected by the growth of the quenching crystals is schematically shown in FIG 7 (Khartcyzov et al. 2022): an increase in the volume of the solid phases will lead to a decrease in the volume of the liquid slag suitable for accurate measurement using the EPMA.
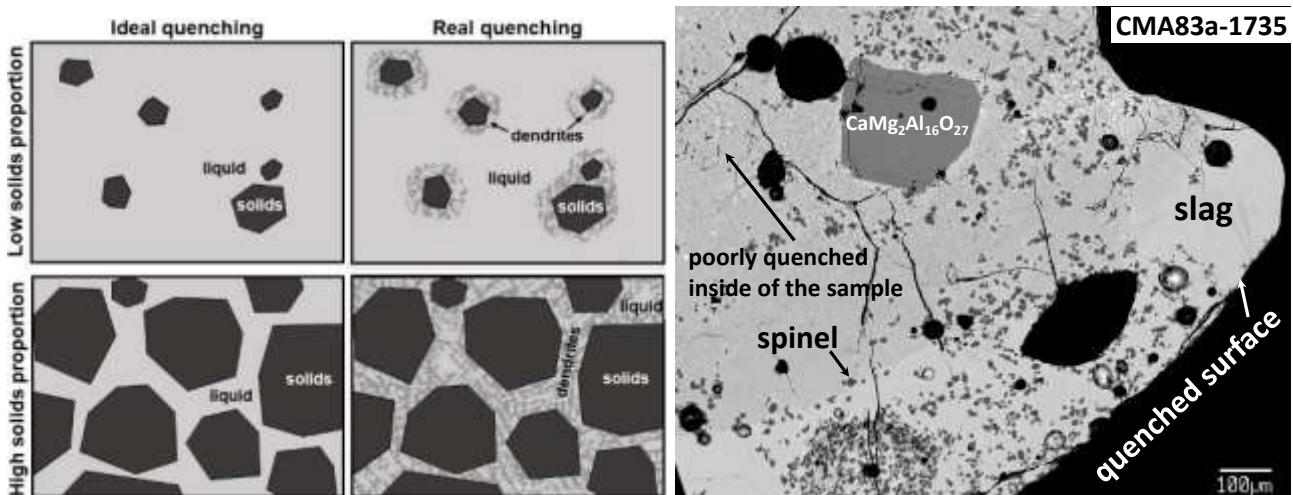
FIG 7 – A schematic diagram illustrating the correlation between the volume fraction of solid phases and the volume fraction of homogenous liquid phase (Khartcyzov et al. 2022), and example of microstructure with well-quenched slag on the surface and poorly quenched inside.

The steps to analyse of micro- and macro- inhomogeneity trends can be summarised as follows:

- Identify all phases. If unsure, use EDS, literature, powder XRD database, first-principles predictions.

- Make a hypothesis of reactions occurring within the sample as it approached the equilibrium. Prove it by varying starting conditions, equilibration time, etc.

- Macro-inhomogeneity check: measure the trend in similar areas across the sample (Hidayat et al. 2023).

- Micro-inhomogeneity check: measure the trends in each location. A distance from solids must be kept as described above and supported by a micrograph.

- In the case of viscous liquid samples, which are at risk of equilibration issue, use areas close and exposed to solids – targets of liquid/solid equilibrium.

- In the case of fluid liquid samples, which are at risk of quenching issue, use liquid areas free from solids, and those first exposed to quenching medium.

- Tune contrast to the maximum to identify inhomogeneities and to find hidden phases.

- Non-equilibrium samples can only be accepted with a special proof that at least local equilibrium exists.

- Average of all measurements is not directly acceptable. Plotting the scattered points compositions against a phase diagram should reveal the existence or absence of a systematic trend. The points that are obviously further from equilibrium / or affected by poor quenching should be rejected, rather than averaged.

Over the years, some issues were identified with the standard EPMA ZAF-correction, used to recalculate X-ray counts into concentrations, considering complex effects of interaction between electrons and the sample, as well as X-rays and the sample. Many uncertainties can be resolved by introduction of secondary standards within the sample. Ideal secondary standard is a stoichiometric compounds existing within the system of interest. Good examples are: $PbSiO_3$, Pb_2SiO_4, Zn_2SiO_4, Fe_2SiO_4, $Ca_2Fe_2O_5$, $CaFe_2O_4$, $CaAl_2O_4$, $FeAl_2O_4$, $CuSiO_3$, $CuAlO_2$, Cu_2PbO_2, etc. (Shevchenko and Jak 2017, 2018, 2019a, 2019b; Shevchenko and Jak 2021; Cheng et al. 2021; Khartcyzov et al. 2023). When secondary standards are not available, using alternative types of ZAF-corrections, such as Mass Absorption Coefficients sets (MACs) were proved to be valuable. Using different EPMA machines for mutual check was tried in many cases. Some trends were revealed for neighbouring elements in Periodic table, e.g. Fe-Al – Co-Al – Ni-Al – Cu-Al – Zn-Al. All of them had stoichiometric compounds (or approaching stoichiometric at certain conditions) – spinel ($FeAl_2O_4$, $CoAl_2O_4$, $NiAl_2O_4$, $ZnAl_2O_4$) and delafossite ($CuAlO_2$). For all of them, the concentrations of Al were overestimated if the existing Mass Absorption Coefficients set was used. Larger overestimation was observed when Al is combined with heavier elements (Cu, Zn) than lighter (Fe, Co). This effect is not universal but depends on the local EPMA machine, software and settings used. Therefore, each machine / software / settings combination needs to be calibrated against stoichiometric compounds, and the correction developed accordingly.

The Secondary X-ray fluorescence is a widely overlooked source of "fake solubility". It is observed for transition elements (Cr, Mn, Fe, Co, Ni, Cu, Zn) in light element-rich phases (SiO_2, CaO, Al_2O_3) (Hidayat, Hayes, and Jak 2012; Hidayat et al. 2012; Xia, Liu, and Taskinen 2016; Hamuyuni, Klemettinen, and Taskinen 2016; Shevchenko and Jak 2018). Interesting cases involved two neighbouring transition element-rich phases inside one another, such as over-estimated % Fe in metallic Cu, which was surrounded by FeO-rich slag. Also, several % overestimation of Cu was noticed in zincite phase (ZnO), which was surrounded by the Cu-rich slag (Shevchenko and Jak 2020a).

The progress in (1) Quantity and selection of studied systems, and (2) Accuracy and reliability of results for each systems has become a foundation for the next stage in thermodynamic modelling. It has allowed gradual improvement of the accuracy of thermodynamic models for all studied systems. But it also revealed some limitations of the thermodynamic models, which could not be resolved without the deep re-assessment of model parameters, and even some concepts of the models themselves. Further in the paper, we describe the revision of properties of all end-members of model solutions.

REVISION OF THERMODYNAMICS OF END-MEMBERS

Since the early development of FactSage solution models, heat capacities of supercooled liquids below melting points were usually assigned the same functions of temperature as the corresponding solid phases. This often resulted in a discontinuous function for the pure liquid heat capacity (Cp) at the melting temperature. Typically, the heat capacity of liquids is about 10% higher compared to the solid of the same composition (FIG 8a). The discontinuity is also present in the heat capacities of multicomponent liquids, which are mostly approximated as an additive sum of all liquid endmembers, with only a minor contribution from the quasichemical interaction. The experimental evidence accumulated later does not support any jumps in liquid heat capacities (Richet and Bottinga 1985;

Richet and Bottinga 1986). Instead, most liquid silicates demonstrate constant heat capacities down to the lowest temperature of their stable existence, which can be closely approximated by the additive sum of liquid endmember heat capacities above their melting points. Moreover, for glass-forming liquids such as SiO_2, constant heat capacity (81.4 J/mol K) is observed down to glass transition point (Richet et al. 1982). The latter point (~1200°C for SiO_2) is not a thermodynamic but a kinetic phenomenon, i.e. shifts to lower temperature on longer time scales and is sensitive to even minor impurities. Therefore, constant high heat capacity for equilibrium (relaxed) supercooled SiO_2 liquid may be extended below 1200°C, but not indefinitely, since the entropy of this supercooled liquid must not become lower than the entropy of the most stable solid at low temperature (low-quartz) – this condition known as "Kauzmann paradox" (Stillinger 1988; Johari 2000; Speedy 2003). While the heat capacity of supercooled SiO_2 can be measured due to its high viscosity, other pure oxide supercooled liquids could not be experimentally obtained, so their heat capacities may only be evaluated from the multicomponent data (Stebbins, Carmichael, and Moret 1984; Lange and Navrotsky 1992). Similarly, the heat capacities of all other supercooled liquid endmembers between ~1000°C and their melting point need to be increased according to the literature for multicomponent melts – for example, for most divalent oxides (CaO, MgO, FeO, ZnO) from 50-60 J/mol K (as in solid phases) to at least 70-80 J/mol K. This allows significant improvement of description of binary and multicomponent phase diagrams while simultaneously removing excessive negative interaction parameters, the only purpose of which was to compensate for underestimated liquid Cps. This compensation, however, can never be perfect and resulted in large discrepancies in slopes of liquidus that would accumulate to >100 K discrepancy in some areas (FIG 8b).
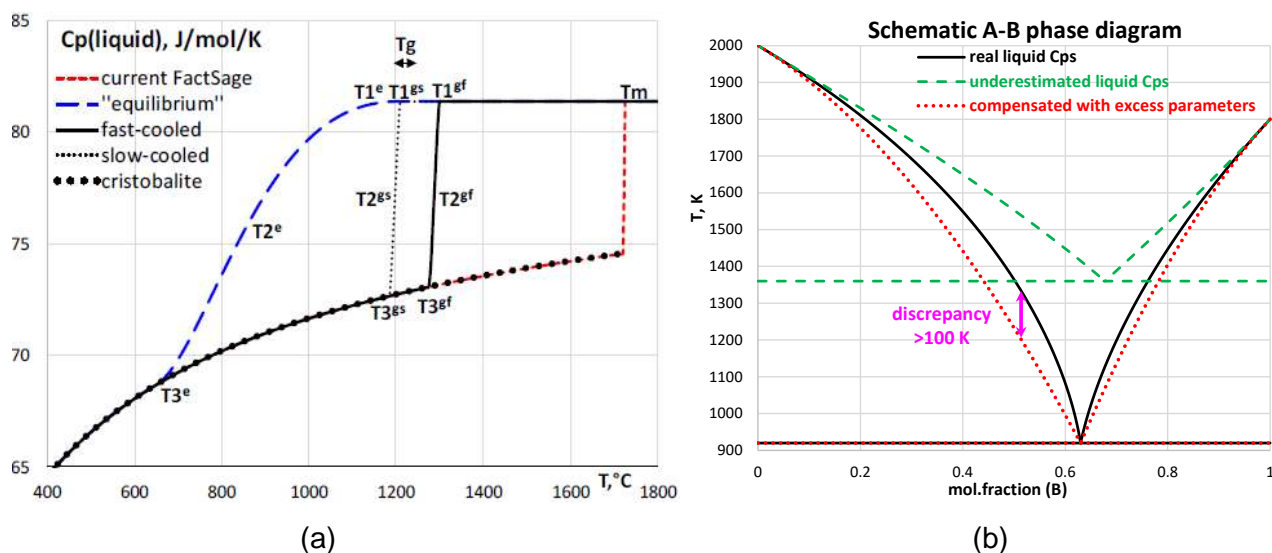
FIG 8 – Example of the supercooled liquid SiO_2 Cp improvement (a), and schematic effect of the liquid endmember Cps on the simple eutectic, ideal liquid solution binary A-B phase diagram (b).

Principles in revision of endmember thermodynamic properties:

1. Heat capacity must be a non-negative, monotonically increasing function on temperature.

(*Unless there is solid experimental evidence of otherwise, e.g. due to magnetic transitions*)

Usually, in the revised version of thermodynamic model, the range 0-50 K is described by

$Cp = aT + bT^2 + cT^3 + dT^4 + eT^5$ (*no terms with T power <1 should be used, to avoid divergence*),

50-298.15K: $Cp = a + bT + cT^2 + dT^3 + eT^4$

298.15-X (X~1000-3000 K): $Cp = a + bT + cT^{-2} + dT^2$ + some other terms if needed

Mandatory term for highest T (X to >6000 K): $Cp = a + bT^{-0.5} + cT^{-1} + dT^{-2} + eT^{-3}$ (*no terms with T power >0 should be used, to avoid divergence*)

2. Heat capacities and entropies of solid allotropes and liquid endmember of the same composition should follow the same sequence as their stability ranges on the temperature scale

– to ensure no unreasonable restabilisation of liquid or high-T solid at low T, or solid at high T.

3. Entropies of all solid and liquid endmembers should (*at least approximately***) tend to 0 at 0 K (3rd law of thermodynamics).**

Although pyrometallurgy rarely encounters T < 25°C, this fundamental principle allowed to fix lots of issues over the last few years.

It is known that glasses / amorphous solids have small residual positive entropy at 0 K. This is due to incomplete relaxation – the viscosity below the glass transition (T_g) becomes so high that the lowest-entropy most-stable state is not achieved below T_g within reasonable experimental timescale. What is known for sure is a) the difference of entropy between supercooled liquid and solid decreases below T_{melt}, and b) it must remain non-negative to avoid "Kauzmann's paradox". There is no consensus in literature whether the entropy of liquid should be exactly 0 at 0 K (Speedy 2003; Benigni 2021), or may remain somewhat higher. There are recent examples of thermodynamic models where zero entropy of supercooled liquid at 0 K is assumed: (Sergeev et al. 2019; Yazhenskikh et al. 2021; Khvan et al. 2018; Khvan et al. 2019; Bigdeli, Chen, and Selleby 2018; Khvan et al. 2020; Bajenova et al. 2020; Khvan et al. 2022; Khvan, Uspenskaya, and Aristova 2024; Li et al. 2017; He and Selleby 2022). While there are different ways to extrapolate the thermodynamic properties of supercooled liquids below their observed glass transitions, they usually result in very similar outcomes, as long as the range between the glass transitions of most endmembers (~400-800°C) and their melting points (1700-2900°C) is described well.

4. Heat capacities and entropies of all chemically similar species should have similar tendencies, with physically sound dependence on the position in Periodic Table.

The currently used liquid slag model describes oxide and sulphide endmembers as unbreakable species (e.g. CaO, FeS), while Matte/Metal – as combinations of metal (e.g. Ca, Fe) + hypothetical liquid O or S.

For example, for trivalent oxides (FIG 9),

- Heat capacities (Cp) of all M_2O_3 liquid endmembers reach ~150-160 J/mol K above 500 K and do not change much anymore.

- Entropies S of all M_2O_3 liquid endmembers have systematic trend on Periodic Table position: low S (light Al) => high S (heavy Bi).

5. A systematic revision has been underway to ensure **both approaches** (i.e. oxide "FeO" in slag and elemental "Fe, O" in matte/metal) result in **consistent** thermodynamic properties over the whole temperature range (0 K – at least 2000 K).

This involved modifying the heat capacity of the hypothetical liquid O endmember in matte/metal to a lower value (29 J/mol K) at high T to avoid spurious formation of "oxide matte" instead of liquid slag for many systems (Pb-O, Sb-O, Bi-O, ...)

6. All endmembers should be reviewed with regards of all recent literature (TABLE 2**, FIG 10).**

Some were inherited from early versions of FactSage (1980-1990s) and appeared to be obsolete.

Systematic analysis of pure oxide endmembers:

- enthalpies/entropies of melting vs T_{melt},

- heat capacities of liquid and solids at T_{melt}

should be consistent throughout the whole Periodic Table (FIG 11).
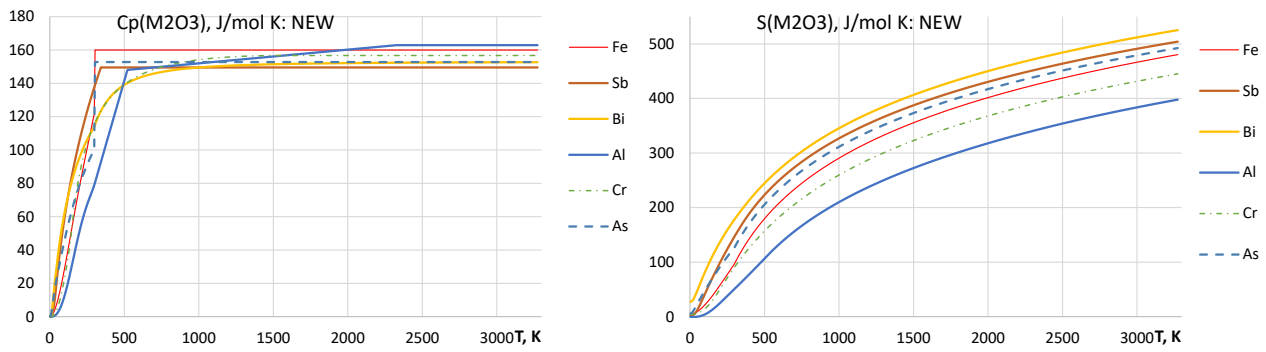
FIG 9 – Systematic change in heat capacities (Cp) and entropies (S) of trivalent liquid slag endmembers (M_2O_3) in the revised thermodynamic model, as function of temperature. All Cps stabilise at 150-160 J/mol K above ~500 K, while the entropies are usually ranked by atomic number (Al<Cr<Fe<As<Sb<Bi).

TABLE 2 – List of updates in the properties of pure components (endmembers) of the oxide database within the recent major thermodynamic revision. Note: properties below 298 K were also described for all solids and liquids.

Component	Changed T_{melt}, ΔH_{melt}	Changed $C_p(liq)$ (J/mol K)	Changed other; reference
SiO_2	-	Increased from 74 to 83	(Wen et al. 2023)
CaO	Increased T_{melt} from 2572 to 2896°C Increased ΔH_{melt} from 79.5 to 83 kJ/mol	Increased from 55 to 80	Increased Cp(solid) > 2000 K
FeO	-	Increased from ~60 to 71	(Wen et al. 2024)
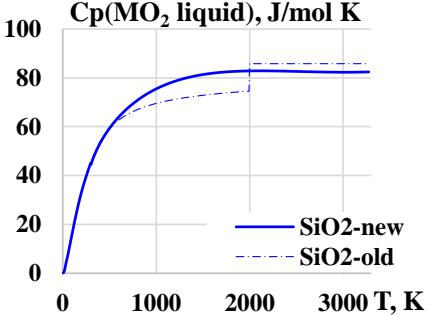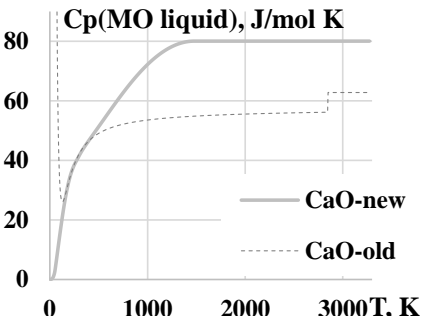
Fe$_2$O$_3$	Decreased T$_{melt}$ from 1695 to 1673°C Increased ΔH$_{melt}$ from 77.2 to 98.6 kJ/mol	Increased from 145 to 160 **Cp(M$_2$O$_3$ liquid), J/mol K** Legend: Fe2O3-new, Fe2O3-old	(Wen et al. 2024)
PbO	Increased ΔH$_{melt}$ from 25.5 to 27.7 kJ/mol	Increased from <60 to 65 **Cp(MO liquid), J/mol K** Legend: PbO-new, PbO-old	(Wen et al. 2023)
ZnO	-	Increased from 55-60 to 70 **Cp(MO liquid), J/mol K** Legend: ZnO-new, ZnO-old	(Wen et al. 2023)
Cu$_2$O	-	Decreased from 120 to 103 **Cp(M$_2$O liquid), J/mol K** Legend: Cu2O-new, Cu2O-old	"Apparent MQM coordination number" from 1 to 2 (Wen et al. 2023)
Al$_2$O$_3$	-	Increased from ~145 to 155-160 **Cp(M$_2$O$_3$ liquid), J/mol K** Legend: Al2O3-new, Al2O3-old	
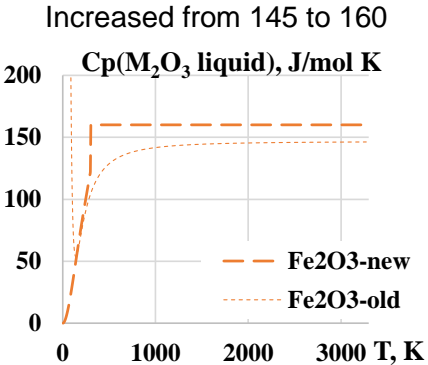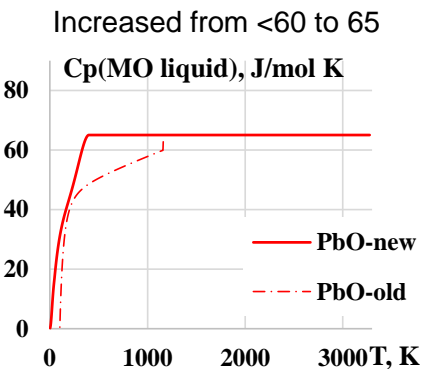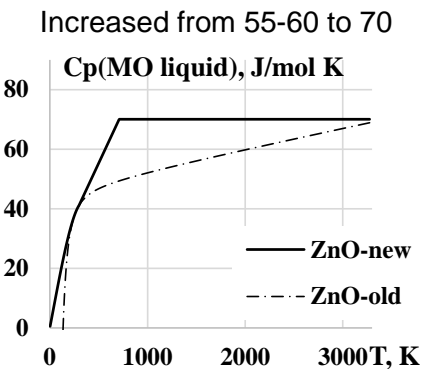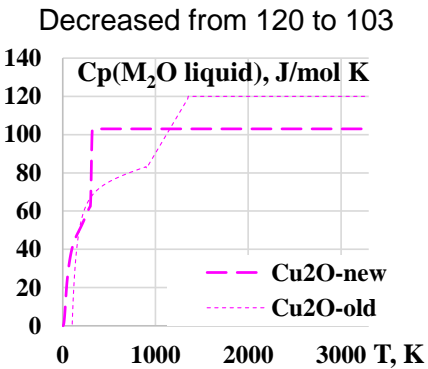
MgO	Increased T_{melt} from 2825 to 2941°C Increased ΔH_{melt} from 77.4 to 85.4 kJ/mol	Increased from ~60 to 72 **Cp(MO liquid), J/mol K** ■ MgO-new ─·─ MgO-old	Increased Cp(solid) > 2000 K Partially published by (Abdeyazdan et al. 2024)
Cr_2O_3	-	Increased from 130-135 to 157 **Cp(M₂O₃ liquid), J/mol K** ── Cr2O3-new ─·─ Cr2O3-old	-
CrO	Increased ΔH_{melt} (from $Cr+Cr_2O_3$)	Increased from ~54 to 72 **Cp(MO liquid), J/mol K** ── CrO-new ─·─ CrO-old	-
As_2O_3		Made smooth below 298 K **Cp(M₂O₃ liquid), J/mol K** ─ ─ As2O3-new ········ As2O3-old	-
As_2O_5	Introduced first time	Set as 205 **Cp(M₂O₅ liquid), J/mol K** ─ ─ As2O5-new	-
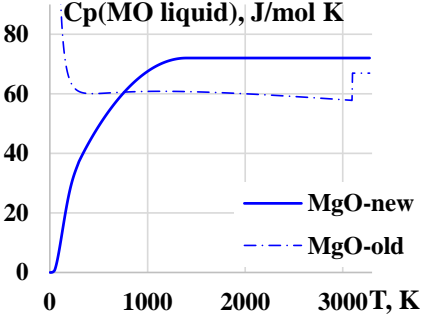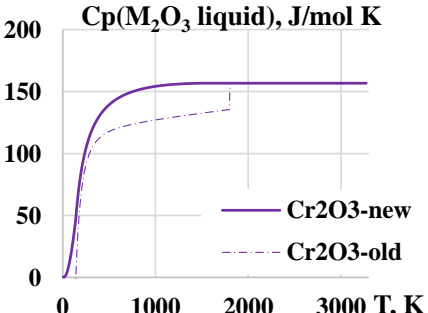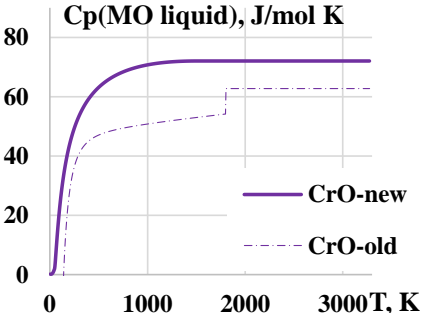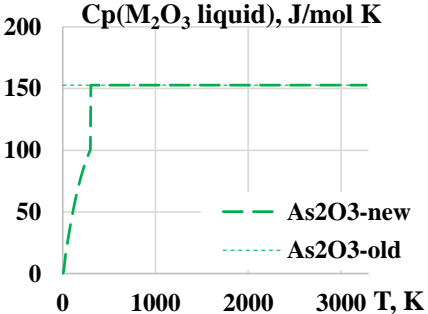
19

SnO	-	Made smooth below 1000 K	Partially published in (Shevchenko et al. 2021)
SnO2	Increased T_{melt} from 1625 to 2349 and then to 2439°C (Note: these are T_{melt} under closed conditions – at finite pO_2 they are lower, currently being set as 2144 at 1 atm O_2 and 2059°C at 0.21 atm O_2) Increased ΔH_{melt} from 41.1 to 49.8 and then to 55.5 kJ/mol	Increased from 92 to 97	Partially published in (Shevchenko et al. 2021)
Sb2O3	-	Decreased from 157 to 150	Revised Cp(solids), ΔH_{form} and $\Delta H_{transition}$ to destabilise Sb_2O_3 liquid
Bi2O3	-	Increased from 140 to 144	-
Ag2O	-	No change	(Sultana, Shevchenko, and Jak 2021)
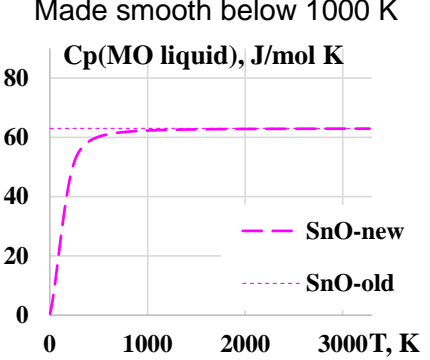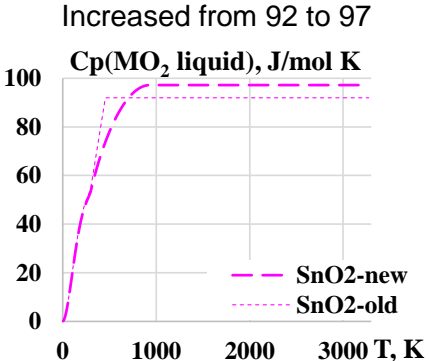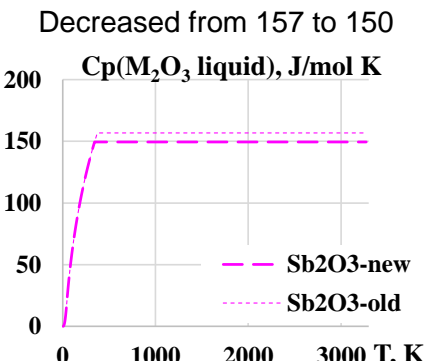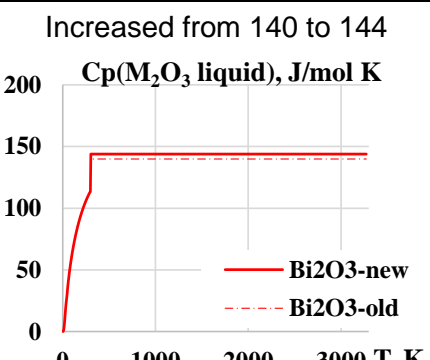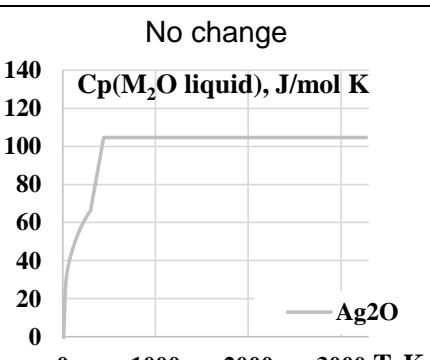
Au$_2$O	-	Decreased from 121 to 103 	-
NiO	Increased T$_{melt}$ from 1955 to 1990 °C (Note: these are T$_{melt}$ under closed conditions – at finite pO$_2$ they are lower, currently being set as 1970 at 1 atm O$_2$ and 1947°C at 0.21 atm O$_2$) Increased ΔH$_{melt}$ from 58.3 to 59.5 kJ/mol	Increased from 67 to 71 	(Abdeyazdan, Shevchenko, and Jak)
CoO	T$_{melt}$ = 1830°C Increased ΔH$_{melt}$ from 40 to 42.1 kJ/mol	Made smooth below 1400 K 	-
Na$_2$O	-	Increased from 99 to 105 	-
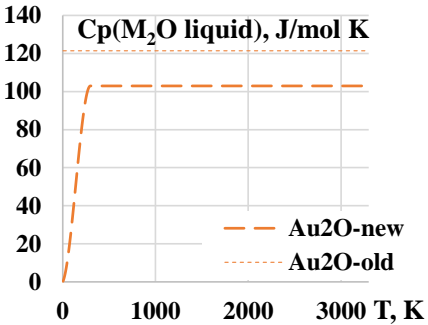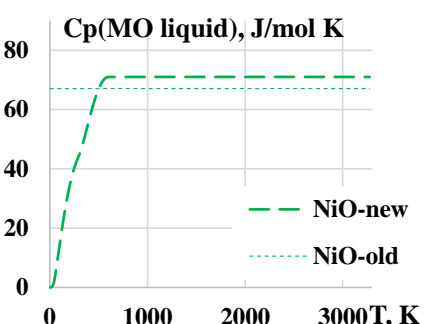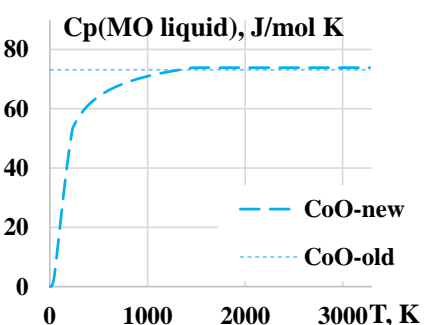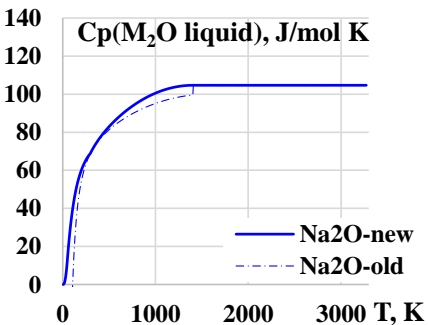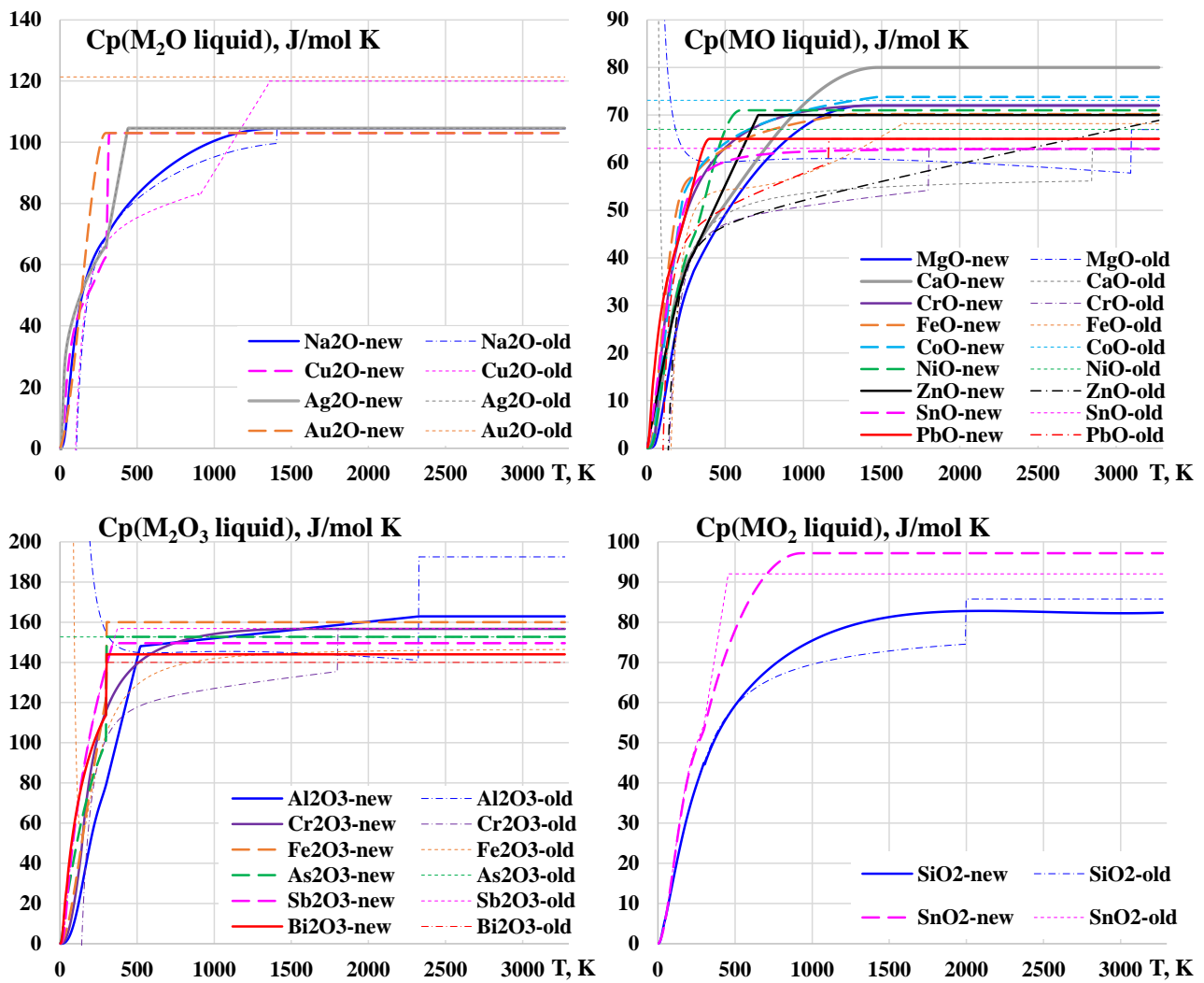
FIG 10 – Comparison of old and new heat capacities of liquid monovalent (M_2O), divalent (MO), trivalent (M_2O_3) and tetravalent (MO_2) liquid slag endmembers. Several unreasonable jumps (Na_2O, CrO, PbO, MgO, CaO, Cr_2O_3, Al_2O_3, SiO_2) and divergences to ±∞ (MgO, CaO, ZnO, Al_2O_3, Fe_2O_3) at low or high T have been corrected.
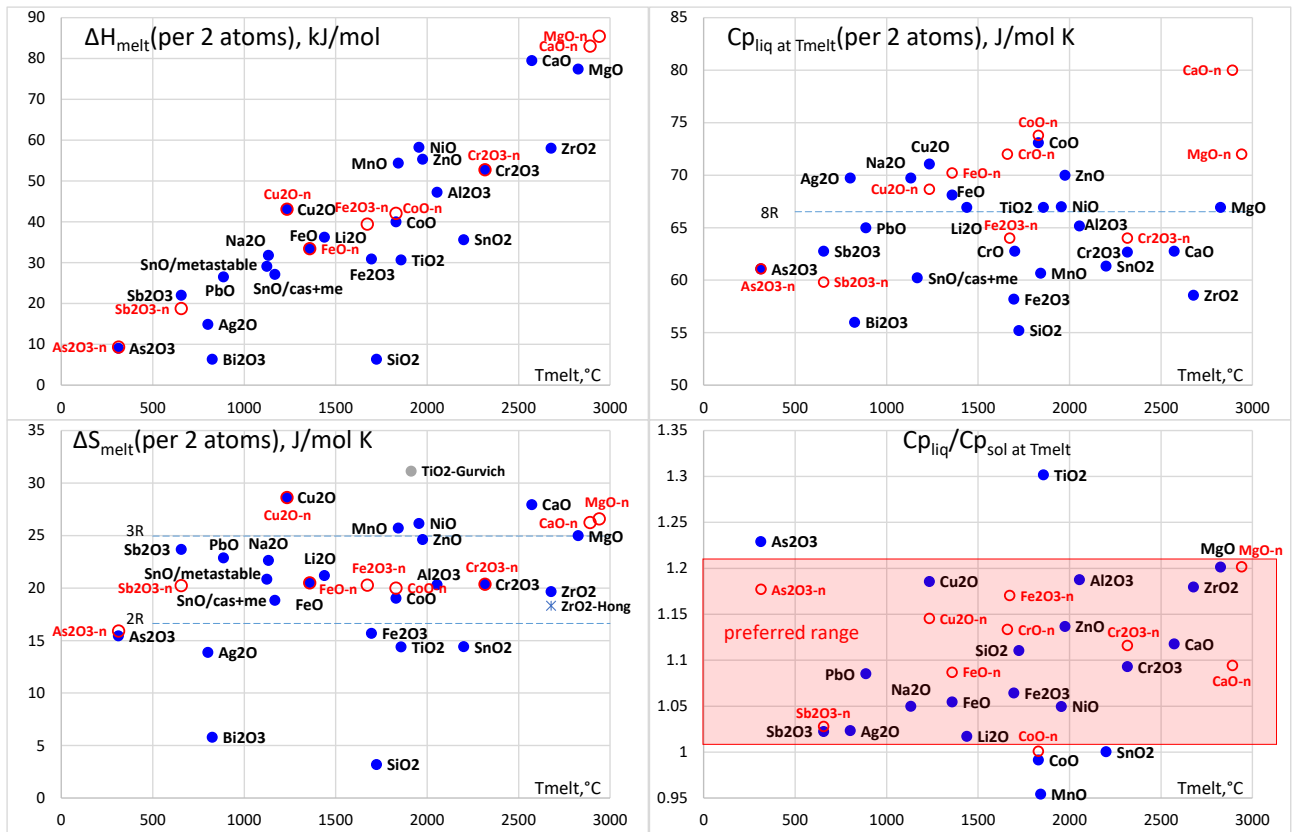
FIG 11 – Comparison of enthalpies of melting (ΔH_{melt}), entropies (ΔS_{melt}), heat capacities of liquids (Cp_{liq} at T_{melt}) and ratios of liquid to solid heat capacities at T_{melt}, all normalised to 2 atoms for presentation purpose. Red circles represent corrected properties for some endmembers (e.g. CaO-n).

Ideally, all elements should have (at least approximately) the same high-T heat capacities when expressed as (oxide – pure liquid O) and as (pure liquid metal) = ideal dashed line (y=x).

Existing discrepancies (FIG 12) provide clues for further improvement of the database robustness, and will make introduction of new species (e.g. As^{5+}, Sb^{5+}, other elements) more fundamentally supported. Note: this chart includes elements that are not in the current thermodynamic database – literature review was undertaken to plot Li^+, P^{5+}, K^+, Ti^{3+}, Ti^{4+}, V^{2+}, V^{3+}, V^{4+}, V^{5+}, Mn^{2+}, Mn^{3+}, Ge^{4+}, Zr^{4+}, Te^{4+}, Ba^{2+} – from public FactSage, etc. – to ensure consistency for all possible elements. Some of them (e.g. P^{5+}, V^{5+}, Te^{4+}, Zr^{4+}) do not align with the principles described here – indicating potential inaccuracies in properties from literature.
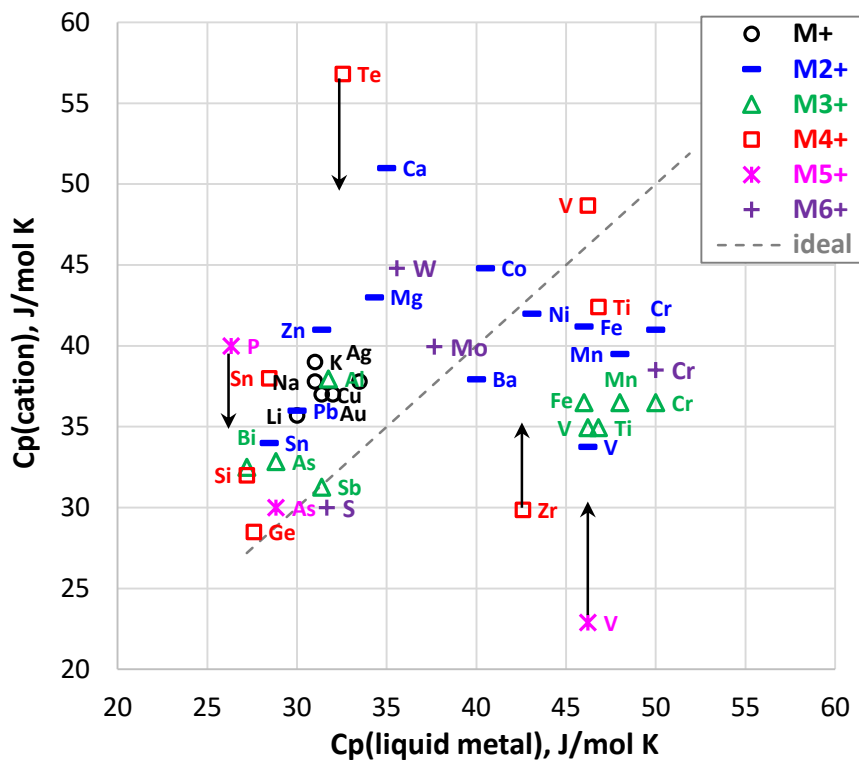
FIG 12 – Correlation between the heat capacities of pure liquid elements (metals and metalloids, e.g. P, Te, S) and their cations in liquid slag, calculated in assumption of $Cp(O^{2-}) = 29$ J/mol K or (for covalently bound in SiO_2, GeO_2, SO_3 groups) 25 J/mol K. Deviations from "ideal" dashed line indicate likely uncertainties in presently accepted Cp of the liquid element and/or its liquid oxide, with arrows showing desired correction.

CONCLUSIONS

Advances in experimental technique and scope within the 20-component Cu-Pb-Zn-Fe-Ca-Al-Mg-Si-O (major) – Cr-Na (slagging) – As-Sn-Sb-Bi-Ag-Au-Ni-Co (minor) slag-solids-metal-matte-speiss-sulphate system have been demonstrated in this paper. Improved range, quantity and accuracy of experimental data have initiated major improvements in thermodynamic model, including revision of properties of pure components (endmembers) that has not been attempted since the 1990s.

ACKNOWLEDGEMENTS

REFERENCES

Abdeyazdan, Hamed, Maksym Shevchenko, Jiang Chen, Peter C. Hayes, and Evgueni Jak. 2024. 'Phase equilibria in the ZnO-MgO-SiO₂ and PbO-ZnO-MgO-SiO₂ systems for characterizing MgO-based refractory - slag interactions', *J. Eur. Ceram. Soc.*, 44: 510-31.

Abdeyazdan, Hamed, Maksym Shevchenko, and Evgueni Jak. 2024. 'Phase equilibria in the NiO-ZnO-SiO$_2$ and PbO-NiO-ZnO-SiO$_2$ systems', *J. Eur. Ceram. Soc.*, 2024:659701, DOI: 10.1016/j.jeurceramsoc.2024.03.028

Bajenova, I., A. Khvan, A. Dinsdale, and A. Kondratiev. 2020. 'Implementation of the extended Einstein and two-state liquid models for thermodynamic description of pure SiO$_2$ at 1 atm', *Calphad*, 68: 101716.

Benigni, P. 2021. 'CALPHAD modeling of the glass transition for a pure substance, coupling thermodynamics and relaxation kinetics', *Calphad*, 72: 102238.

Bigdeli, Sedigheh, Qing Chen, and Malin Selleby. 2018. 'A New Description of Pure C in Developing the Third Generation of Calphad Databases', *J. Phase Equilib. Diffus.*, 39: 832-40.

Cheng, Siyu, Maksym Shevchenko, Peter C. Hayes, and Evgueni Jak. 2021. 'Experimental Phase Equilibria Studies in the FeO-Fe$_2$O$_3$-CaO-SiO$_2$ System and the Subsystems CaO-SiO$_2$, FeO-Fe$_2$O$_3$-SiO$_2$ in Air', *Metall. Mater. Trans. B*, 52: 1891-914.

Hamuyuni, Joseph, Lassi Klemettinen, and Pekka Taskinen. 2016. 'Experimental phase equilibrium data of the system Cu-O-CaO-Al$_2$O$_3$ at copper saturation', *Calphad*, 55: 199-207.

He, Zhangting, and Malin Selleby. 2022. 'A third generation Calphad description of W-C including a revision of liquid C', *Calphad*, 78: 102449.

Hidayat, T., A. Fallah Mehrjardi, M. Shevchenko, P. C. Hayes, and E. Jak. 2023. 'Development of Experimental Techniques for the Phase Equilibrium Study in the Pb-Fe-O-S-Si System Involving Gas, Slag, Matte, Lead Metal and Tridymite Phases', *Processes*, 11: 372.

Hidayat, T., H. M. Henao, P. C. Hayes, and E. Jak. 2012. 'Phase Equilibria Studies of the Cu-Fe-O-Si System in Equilibrium with Air and with Metallic Copper', *Metall. Mater. Trans. B*, 43: 1034-45.

Hidayat, Taufiq, Peter C. Hayes, and Evgueni Jak. 2012. 'Experimental Study of Ferrous Calcium Silicate Slags: Phase Equilibria at Between 10^{-8} atm and 10^{-9} atm', *Metall. Mater. Trans. B*, 43: 27-38.

Jak, E. 2018. "The role of research in pyrometallurgy technology development - from fundamentals to process improvements - Future, Sulphide Smelting." In *Extraction 18*. Ottawa, Canada: TMS/CIM.

Jak, E. , T. Hidayat, D. Shishin, A. F. Mehrjardi, J. Chen, S. A. Decterov, and P. Hayes. 2016. "Integrated experimental and modelling research for non-ferrous smelting and recycling systems." In *Proc. 10th International Conference on Molten Slags, Fluxes and Salts (Molten16)*, edited by R. G. Reddy, P. C. Chaubal, P. C. Pistorius and Uday B. Pal, 947-59. Seattle, Washington, USA.

Jak, E., and P. C. Hayes. 2002a. 'Experimental Liquidus in the PbO-ZnO-"Fe$_2$O$_3$"-(CaO+SiO$_2$) System in Air, with CaO/SiO$_2$=0.35 and PbO/(CaO+SiO$_2$)=3.2', *Metall. Mater. Trans. B*, 33B: 851-63.

———. 2002b. 'Experimental Study of Phase Equilibria in the PbO-ZnO-"Fe$_2$O$_3$"-CaO-SiO$_2$ System in Air for High Lead Smelting Slags (CaO/SiO$_2$=0.35 and PbO/(CaO+SiO$_2$)=5.0 by Weight)', *Metall. Mater. Trans. B*, 33B: 817-25.

Jak, Evgueni. 2012. "Integrated experimental and thermodynamic modelling research methodology for metallurgical slags with examples in the copper production field " In *9th Intl. Conf. on Molten Slags, Fluxes and Salts*, W077, 1-28. Beijing, China: The Chinese Society for Metals.

Jak, Evgueni, Peter C. Hayes, and Hae-Geon Lee. 1995. 'Improved methodologies for the determination of high temperature phase equilibria', *Korean Journal of Minerals and Materials Institute (Seoul)*, 1: 1-8.

Jak, Evgueni, Maksym Shevchenko, Denis Shishin, Evgenii Nekhoroshev, Jiang Chen, and Peter Hayes. 2024. "University Research on molten slags, matte, speiss and metal systems for high temperature processing." In *Molten 2024*. Brisbane.

Jak, Evgueni, Denis Shishin, Maksym Shevchenko, and Peter Hayes. 2022. "Integrated Experimental Phase Equilibria and Thermodynamic Modelling Research and Implementation in Support of Pyrometallurgical Copper Processing." In *COPPER 2022*. Santiago, Chile.

Johari, G. P. 2000. 'An equilibrium supercooled liquid's entropy and enthalpy in the Kauzmann and the third law extrapolations, and a proposed experimental resolution', *J. Chem. Phys.*, 113: 751-61.

Khartcyzov, Georgii, Maksym Shevchenko, Siyu Cheng, Peter C. Hayes, and Evgueni Jak. 2022. 'Experimental phase equilibria studies in the "$CuO_{0.5}$"-CaO-SiO_2 ternary system in equilibrium with metallic copper', *Ceram. Int.*, 48: 9927-38.

———. 2023. 'Experimental phase equilibria study and thermodynamic modelling of the "$CuO_{0.5}$"-$AlO_{1.5}$-SiO_2 ternary system in equilibrium with metallic copper', *Ceram. Int.*, 49: 11513-28.

Khvan, A. V., T. Babkina, A. T. Dinsdale, I. A. Uspenskaya, I. V. Fartushna, A. I. Druzhinina, A. B. Syzdykova, M. P. Belov, and I. A. Abrikosov. 2019. 'Thermodynamic properties of tin: Part I Experimental investigation, ab-initio modelling of α-, β-phase and a thermodynamic description for pure metal in solid and liquid state from 0 K', *Calphad*, 65: 50-72.

Khvan, A. V., A. T. Dinsdale, I. A. Uspenskaya, M. Zhilin, T. Babkina, and A. M. Phiri. 2018. 'A thermodynamic description of data for pure Pb from 0 K using the expanded Einstein model for the solid and the two state model for the liquid phase', *Calphad*, 60: 144-55.

Khvan, A. V., N. Konstantinova, I. A. Uspenskaya, A. T. Dinsdale, A. I. Druzhinina, A. Ivanov, and I. Bajenova. 2022. 'A description of the thermodynamic properties of pure indium in the solid and liquid states from 0 K', *Calphad*, 79: 102484.

Khvan, A. V., I. A. Uspenskaya, and N. M. Aristova. 2024. 'Critical assessment of the data for Pure Cu from 0 K, using two-state model for the description of the liquid phase', *Calphad*, 84: 102637.

Khvan, A. V., I. A. Uspenskaya, N. M. Aristova, Q. Chen, G. Trimarchi, N. M. Konstantinova, and A. T. Dinsdale. 2020. 'Description of the thermodynamic properties of pure gold in the solid and liquid states from 0 K', *Calphad*, 68: 101724.

Lange, Rebecca A., and Alexandra Navrotsky. 1992. 'Heat capacities of iron(3+) oxide-bearing silicate liquids', *Contrib. Mineral. Petrol.*, 110: 311-20.

Li, Zhou, Sedigheh Bigdeli, Huahai Mao, Qing Chen, and Malin Selleby. 2017. 'Thermodynamic evaluation of pure Co for the third generation of thermodynamic databases', *Phys. Status Solidi B*, 254: 1600231.

Luty, Wacław. 1992. 'Types of Cooling Media and Their Properties.' in Božidar Liščić, Hans M. Tensi and Wacław Luty (eds.), *Theory and Technology of Quenching: A Handbook* (Springer Berlin Heidelberg: Berlin, Heidelberg).

Pizetta Zordão, L. H., V. A. Oliveira, G. E. Totten, and L. C.F. Canale. 2019. 'Quenching power of aqueous salt solution', *Int. J. Heat Mass Transf.*, 140: 807-18.

Richet, P., and Y. Bottinga. 1986. 'Thermochemical Properties of Silicate Glasses and Liquids: A Review', *Rev. Geophys.*, 24: 1-25.

Richet, P., Y. Bottinga, L. Denielou, J. P. Petitet, and C. Tequi. 1982. 'Thermodynamic properties of quartz, cristobalite and amorphous SiO_2: drop calorimetry measurements between 1000 and 1800 K and a review from 0 to 2000 K', *Geochim. Cosmochim. Acta*, 46: 2639-58.

Richet, Pascal, and Yan Bottinga. 1985. 'Heat capacity of aluminium-free liquid silicates', *Geochim. Cosmochim. Acta*, 49: 471-86.

Sergeev, D., B. H. Reis, I. Dreger, M. to Baben, K. Hack, and M. Mueller. 2019. 'Thermodynamics of the $Ca(NO_3)_2$ - $NaNO_3$ system', *Calphad*, 67: 101688.

Shevchenko, M., L. Chen, and E. Jak. 2021. 'Experimental phase equilibria study and thermodynamic modelling of the PbO-"FeO"-SiO_2-ZnO, PbO-"FeO"-SiO_2-Al_2O_3 and PbO-"FeO"-SiO_2-MgO systems in equilibrium with metallic Pb and Fe', *Ceram. Int.*, 48: 15124-35.

Shevchenko, M., T. Hidayat, P. Hayes, and E. Jak. 2016. "Liquidus of "FeO"-SiO_2-PbO slags in equilibrium with air and with metallic lead." In *10th Intl. Conf. on Molten Slags, Fluxes and Salts*, 1221-28. Seattle, Washington, USA.

Shevchenko, M., and E. Jak. 2017. 'Experimental Phase Equilibria Studies of the PbO-SiO_2 System', *J. Am. Ceram. Soc*, 101: 458-71.

———. 2018. 'Experimental Liquidus Studies of the Pb-Fe-Si-O System in Equilibrium with Metallic Pb', *Metall. Mater. Trans. B*, 49: 159-80.

———. 2019a. 'Experimental Liquidus Studies of the Binary Pb-Cu-O and Ternary Pb-Cu-Si-O Systems in Equilibrium with Metallic Pb-Cu Alloys', *J. Phase Equilib. Diff.*, 40: 671–85.

———. 2019b. 'Experimental Liquidus Studies of the Pb-Fe-Ca-O System in air', *J. Phase Equilib. Diff.*, 40: 128-37.

———. 2020a. 'Experimental Liquidus Studies of the ZnO-"$CuO_{0.5}$" and ZnO-"$CuO_{0.5}$"-SiO_2 Liquidus in Equilibrium with Cu-Zn Metal', *J. Phase Equilib. Diff.*, 41: 207-17.

———. 2020b. 'Experimental study and thermodynamic optimization of the ZnO-FeO-Fe_2O_3-CaO-SiO_2 system', *CALPHAD Comput. Coupling Phase Diagrams Thermochem.*, 71: 102011.

Shevchenko, Maksym, A. Ilyushechkin, Hamed Abdeyazdan, and E. Jak. 2021. 'Integrated experimental phase equilibria study and thermodynamic modelling of the PbO-SnO-SnO_2-SiO_2 system in air and in equilibrium with Pb-Sn metal', *J. Alloys Compd.*, 888: 161402.

Shevchenko, Maksym, and Evgueni Jak. 2021. 'Integrated experimental phase equilibria study and thermodynamic modelling of the binary ZnO-Al_2O_3, ZnO-SiO_2, Al_2O_3-SiO_2 and ternary ZnO-Al_2O_3-SiO_2 systems', *Ceramics International*, 47: 20974-91.

Speedy, Robin J. 2003. 'Kauzmann's paradox and the glass transition', *Biophys. Chem.*, 105: 411-20.

Stebbins, J. F., O. S. E. Carmichael, and L. K. Moret. 1984. 'Heat Capacities and Entropies of Silicate Liquids and Glasses', *Contrib. Mineral. Petrol.*, 86: 131-48.

Stillinger, Frank H. 1988. 'Supercooled liquids, glass transitions, and the Kauzmann paradox', *J. Chem. Phys.*, 88: 7818-25.

Sultana, U., M. Shevchenko, and E. Jak. 2021. 'Integrated Experimental Liquidus and Modelling Studies of the Ternary $AgO_{0.5}$-$FeO_{1.5}$-SiO_2 Systems in Equilibrium with Metallic Ag', *Journal of Alloys and Compounds*, 870: 159333.

Wen, X., M. Shevchenko, E. Nekhoroshev, and E. Jak. 2023. 'Phase equilibria and thermodynamic modelling of the PbO–ZnO-"$CuO_{0.5}$"-SiO_2 system', *Ceram. Int.*, 2024:10405, DOI: 10.1016/j.ceramint.2023.12.207

———. 2024. 'Phase Equilibria and Thermodynamic Modelling of the PbO-ZnO-FeO-FeO1.5-SiO_2 system and its subsystems in equilibrium with air/metallic lead/iron', *Ceram. Int.*, 50: 8917-51.

Xia, Longgong, Zhihong Liu, and Pekka Antero Taskinen. 2016. 'Equilibrium study of the Cu-O-SiO_2 system at various oxygen partial pressures', *J. Chem. Thermodyn.*, 98: 126-34.

Yazhenskikh, Elena, Tatjana Jantzen, Dietmar Kobertz, Klaus Hack, and Michael Mueller. 2021. 'Critical thermodynamic evaluation of the binary sub-systems of the core sulphate system Na_2SO_4-K_2SO_4-$MgSO_4$-$CaSO_4$', *Calphad*, 72: 102234.